phys. stat. sol. (b) **233**, No. 3, 416–426 (2002)

Single-Qubit Operations with the Nitrogen-Vacancy Center in Diamond

T. A. KENNEDY[1]) (a), F. T. CHARNOCK[*]) (a), J. S. COLTON (a), J. E. BUTLER (a), R. C. LINARES (b), and P. J. DOERING (b)

(a) Naval Research Laboratory, Washington, DC 20375, USA

(b) Apollo Diamond, Sherbourne, MA 01770, USA

(Received May 13, 2002; accepted July 22, 2002)

PACS: 03.67.Lx; 76.30.–v; 81.05.Uw

A concept combining optics and microwave pulses with the negative charge-state of the nitrogen-vacancy (NV^-) center in diamond is demonstrated through experiments that are equivalent to single-qubit gates, and decoherence for this qubit is examined. The spin levels of the ground state provide the two-level system. Optical excitation provides polarization of these states. The polarized state is operated coherently by 35 GHz microwave pulses. The final state is read out through the photoluminescence intensity. Decoherence arises from different sources for different samples. For high-pressure, high-temperature synthetic diamonds, the high concentration of substitutional N limits the phase-memory to a few μs. In a single-crystal CVD diamond, the phase memory time is at least 32 μs at 100 K. ^{14}N is tightly coupled to the electronic spin and produces modulation of the electron–spin echo decay under certain conditions. A two-qubit gate is proposed using this nuclear spin. This demonstration provides a great deal of insight into quantum devices in the solid state with some possibility for real application.

1. Introduction The nitrogen-vacancy center in its negative charge-state (NV^-) in diamond is a defect/host system with remarkable properties. Its optical transition and spin were established through optical studies and EPR [1, 2]. A long spin lifetime and more details of the energy levels were obtained through Optically Detected Magnetic Resonance (ODMR) and Raman heterodyne spectroscopy at zero and small magnetic fields [3, 4]. These studies and others confirmed that the center has a strong optical transition and a long-lived spin with $S = 1$ in the ground state. Many further experiments have been performed including room temperature ODMR of single NV^- centers [5].

The strong optical transition, long spin lifetimes, and stability of NV^- in diamond have led naturally to concepts and demonstrations aimed at quantum information technology. One approach employs the ^{13}C nuclear spins as qubits with radio-frequency pulses as gates to implement a quantum computer [6]. A second approach makes use of cavity dark states for quantum computing [7]. Other works use the NV^- center as a single-photon source for application in quantum communication [8, 9].

In this work, a concept is demonstrated that uses the electronic spin of the NV^- in diamond as the qubit with optical polarization, microwave pulses as operators, and optical emission for readout. Gates involving a single qubit are demonstrated with ensembles of NV^- centers. Previous work with one sample [10] has been extended to a set of samples, and some of the causes of decoherence can now be given. The involvement of

[1]) Corresponding author; Tel.: +1-202-767-2917; Fax: +1-202-767-1165; e-mail: kennedy@bloch.nrl.navy.mil

[*]) Present address: NIST, Boulder CO, USA.

 0370-1972/02/23310-0416 $ 17.50+.50/0

the ^{14}N nuclear spin is described and a proposal for a two-qubit gate is discussed. Extensions to many qubits through this route are challenging due to the current limits of electronic technology with this center in diamond. Despite this drawback, the realization described provides a great deal of insight into quantum devices in the solid state with some possibility for real application.

This paper is organized as follows. Section 2 describes the concept and demonstration using the NV^- spin and establishes a connection with the criteria for solid-state quantum computing [11]. Section 3 covers the technological issues including decoherence for different samples, the ^{14}N nuclear spin and a two-qubit gate, and scaling to many gates. Section 4 is a summary.

2. Concept and Demonstration of Single-Qubit Gates The concept for quantum computing (QC) can be described by making connections to the five criteria for implementing QC in the solid state [11]. First, the well-defined Hilbert space is implemented with a pair of the electronic spin states from the electronic ground state of NV^- which has $S = 1$. Second, preparation in a particular state is provided by optical polarization that produces a strong population in the $M_S = 0$ state. Third, a low decoherence rate arises from the properties of NV^- in diamond. Fourth, available gate operations are provided by microwave pulses at 35 GHz. The fifth criterion, single-quantum measurements, has not been realized in these experiments which make use of ensembles. However, single quantum (single defect) experiments have been performed [5], and the extension to single defect coherent measurements seems possible [12].

The experiments that demonstrate this concept can now be described following as closely as possible the criteria described above.

Optically exciting the NV^- center at a high rate produces a spin polarization in the ground state [2, 13]. Green light at 2.33 eV is absorbed by NV^- by the ^{3}A to ^{3}E transition, which is broadened by vibronic coupling (Fig. 1a). For these experiments, 400 mW

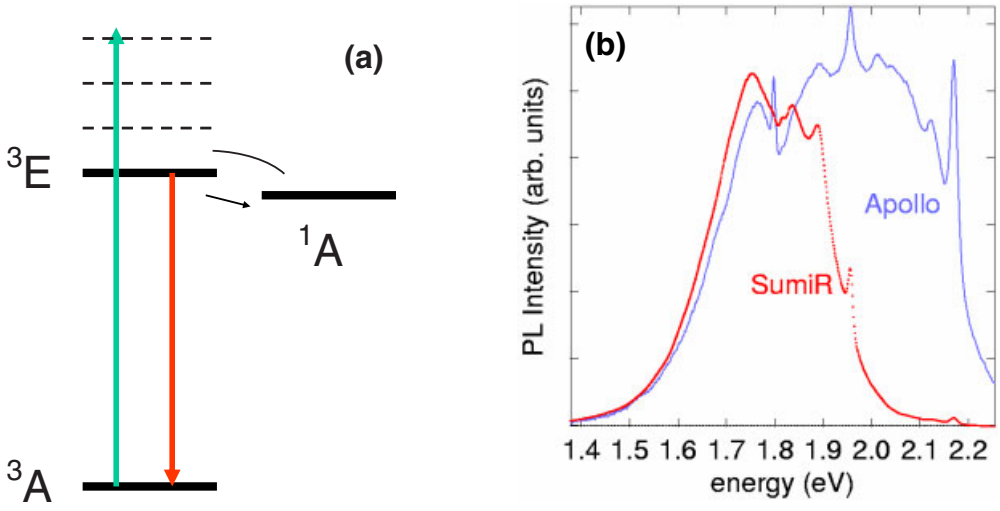

Fig. 1 (online colour). a) Schematic diagram of the optical energy levels for the NV^- center; b) photoluminescence spectra for two diamond samples. In part b), the Apollo diamond shows emission from both charge states of NV while in the SumiR sample the emission from NV^- is dominant

was used, focused to about 100 μm. Most of the time, the excitation decays non-radiatively to the bottom of the ^{3}E state and then recombines radiatively to the ground state at a rate of about 100 MHz. The NV$^-$ emission is also broadened by vibronic coupling (Fig. 1b). This entire process is spin conserving. However, there is a metastable singlet state (^{1}A) at an energy just below the ^{3}E to which the excitation transfers part of the time. The rate to this state is 2 MHz and the process back to the ^{3}E is thermally activated at high temperature and driven by the green light (through another excited state) at low temperature. This process does not conserve spin and leads to a spin polarization of the ground state. The population of the $M_S = 0$ state is enhanced at a rate of 1 kHz under our conditions. The inverse of this is T_1', the time it takes to set the initial state and thus the repetition period for the experiments.

Once there is a spin polarization of the ground state, it can be detected optically through the intensity of the emission since the rate for the optical cycle depends on the spin state. For these experiments, the emission at wavelengths longer than 600 nm (energies less than 2.1 eV) is selected with a filter and detected with a Si photodiode. This

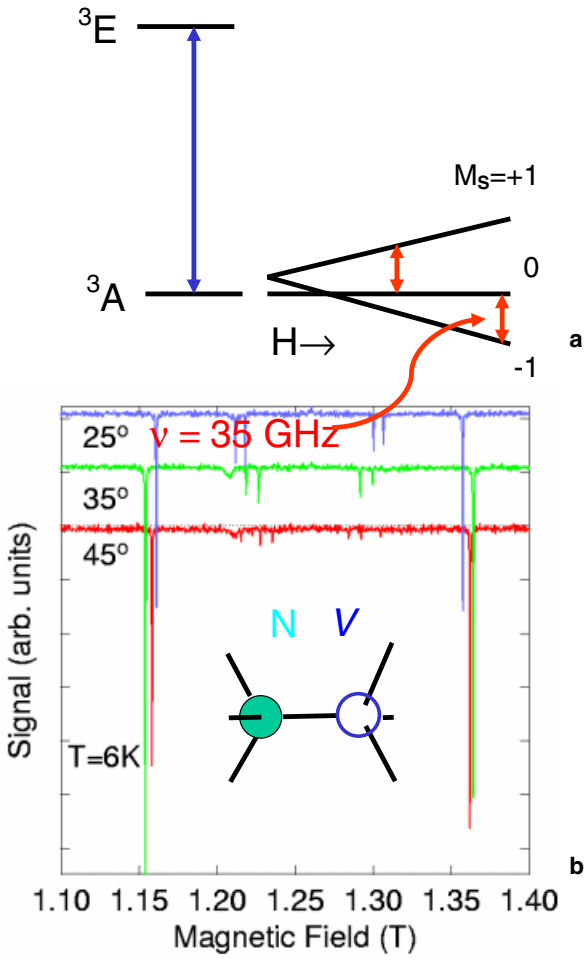

Fig. 2 (online colour). a) Schematic diagram of the energy levels with fine-structure and Zeeman splitting of the ground state; b) ODMR spectra of NV$^-$ for the Apollo sample for three different magnetic-field angles near the [111]. The inset in b) shows the structure of the NV center

selects the NV^- emission from the NV^0 emission in the case of the Apollo CVD sample (Fig. 1b).

With the spins polarized and their state detectable, the electronic spin transitions can be located by ODMR. Some details arising from the symmetry of the centers must be accounted to locate the states. The NV-center consists of a nitrogen impurity in a carbon lattice position next to a vacancy of a carbon atom in the diamond lattice (inset to Fig. 2b). Each NV-center has its axis along one of the four bond directions. The axial symmetry introduces a splitting of the ground state even at zero field (Fig. 2a). Applying a magnetic field of around 1 T produces a Zeeman splitting larger than the zero-field splitting. The OMDR is detectable when the microwave energy matches a transition and destroys the polarization. Rotations of the sample for angles near the [111] direction produce the spectra seen in Fig. 2b. The widely split pair of lines arises from the centers with their axes nearly parallel to [111] while the other centers give rise to pairs of lines with smaller splittings. Selecting either the highest-field ($M_S = 0$ to -1) or lowest-field ($M_S = 0$ to $+1$) line gives a pair of states with which coherent operations can be explored.

The simplest operation is the NOT gate in which the spin is flipped from one eigenstate to the other. The microwave pulse needed for this operator, a π-pulse, can be found by performing transient nutation or Rabi flopping experiments. In these experiments, microwave fields produced by a Gunn oscillator were amplified with a traveling-wave-tube and the switching was done with a fast PIN diode. The Rabi oscillations reveal times from 20 to 400 ns for a π-pulse for different microwave powers (Fig. 3).

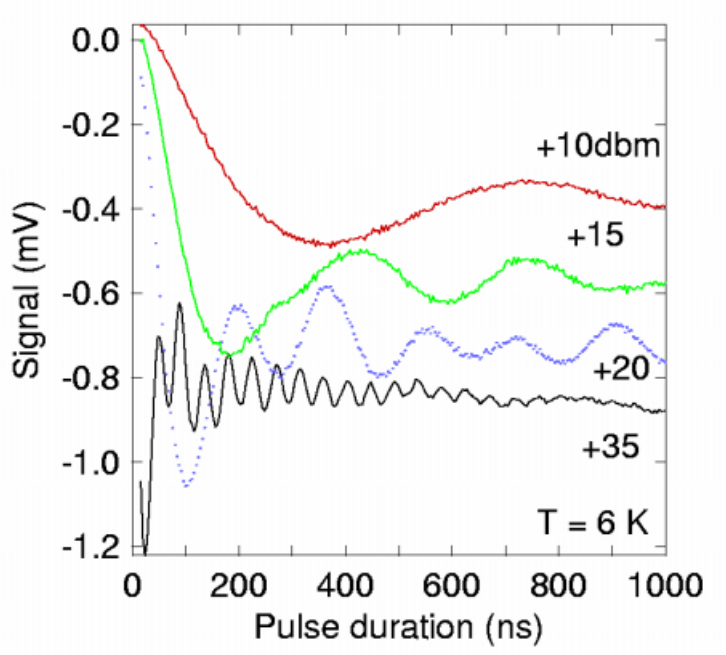

Fig. 3 (online colour). Rabi oscillations or transient nutation for different levels of microwave power. Population inversion occurs for times as short as 20 ns

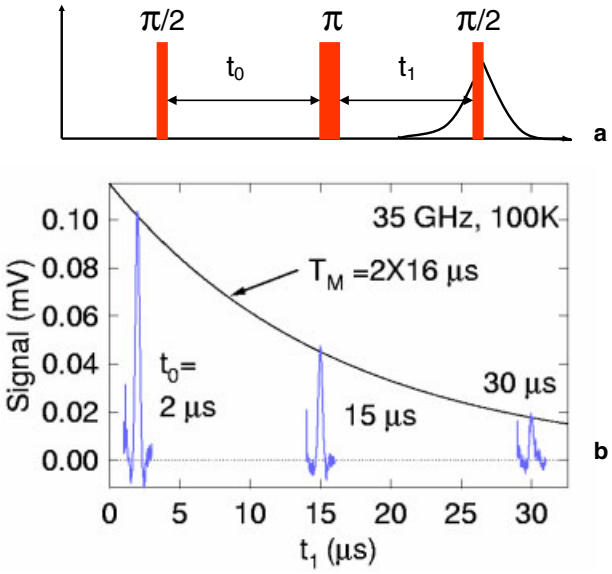

Fig. 4 (online colour). a) Schematic of the electron–spin echo process; b) echoes for three different initial delays t_0. The exponential curve shows that the decay falls to $1/e$ for $t_1 = 16$ µs. Thus, the phase-memory time for this sample is 32 µs

A second operation is the two-pulse or Hahn echo. This operation is important to quantum computation since it provides "refocusing" that allows the control of interactions between distinct qubits [14]. For the present ensemble measurements, the Hahn echo provides the phase-memory time for the NV^- states. In this operation, a $\pi/2$ pulse produces a coherence that is allowed to evolve for a time t_0, a π-pulse inverts the ensemble which, apart from decoherence, refocuses after a second evolution period equal to the first ($t_1 = t_0$). For optical detection, a third pulse is required that converts the remaining coherence to a population (see Fig. 4). The phase-memory time (T_M) is defined as the time from the initial pulse that it takes for the echo to fall to $1/e$ of its initial value. For the Apollo diamond sample, a phase-memory time of 32 µs is measured at temperatures from 1.5 to 100 K. Since this time is close to the limit of the stability of the oscillator and of the magnetic field, it must be regarded as a lower limit for the true phase-memory time in this sample.

3. Technological Issues

3.1 Decoherence The phase-memory observed through the electron–spin echoes in this demonstration is gradually lost through spin–spin interactions between a particular NV^- spin and any nearby other spins. Therefore, in order to probe the exact causes of decoherence the defect identities and concentrations for the different diamond samples have to be analyzed. Fortunately, a lot is known about defects in diamond [15]. The important paramagnetic defects are expected to be other NV^- centers, substitutional nitrogen impurities (N_S), and the spin 1/2 nuclei of the ^{13}C isotopes present at a natural abundance of about 1%.

These defects can influence the NV^- resonance in a variety of ways [16]. First, one must differentiate between static interactions that produce the inhomogeneous broadening seen in the CW spectrum and fluctuations in the interactions that determine the phase-memory. Often the static broadening exceeds the homogeneous width, which is

given by the Fourier transform of the echo envelope. Second, among the dynamic interactions one differentiates the spins in resonance (whose range is determined by the amplitude of the microwave field, H_1), that are called A-spins, from the spins not in resonance, called B spins. In the present case, a subset of the NV^- constitutes the A spins and the other NV^-, the N_S and the nuclei with spin are B spins.

The interaction responsible for each of the couplings is the dipole–dipole interaction that varies as $1/r^3$. If the concentrations of A and B spins are about equal, the A type spins will dominate the relaxation because their interaction is resonant. However, often the concentration of the B spins is larger than that of the A spins, and B spins relax the phase. Calculations of the phase-memory are possible in some limits, but tend to be inaccurate due to the lack of knowledge of the exact defect distribution of the spins coupled with the strong dependence of the interaction on distance. Some simplification is possible as follows. The average inter-defect distance is proportional to the inverse of the cube root of the concentration. Coupled with the dependence of the dipolar interaction on distance ($1/r^3$), this leads to a very simple law for each type of spin:

$$1/T_M = k \times [X] \,, \tag{1}$$

where T_M is the phase-memory time, k is a constant to be determined empirically and [X] is the concentration of the X-spins producing relaxation.

Five samples with different defect concentrations have been studied to elucidate some aspects of the decoherence of NV^- in diamond. These allowed exploration of the effects of the NV^- centers themselves and the substitutional N.

High-pressure, high-temperature (HPHT) grown diamonds often contain a large concentration of N_S with a low, often undetectable, concentration of NV centers. Electron-irradiation of these samples produces vacancies. NV centers can then be formed by annealing the irradiated samples at 800 °C which causes the vacancies to migrate and become trapped next to nitrogen impurities. Photoluminescence then reveals a large NV^- concentration as the Fermi level remains high and preferentially produces the negative charge state (Fig. 5).

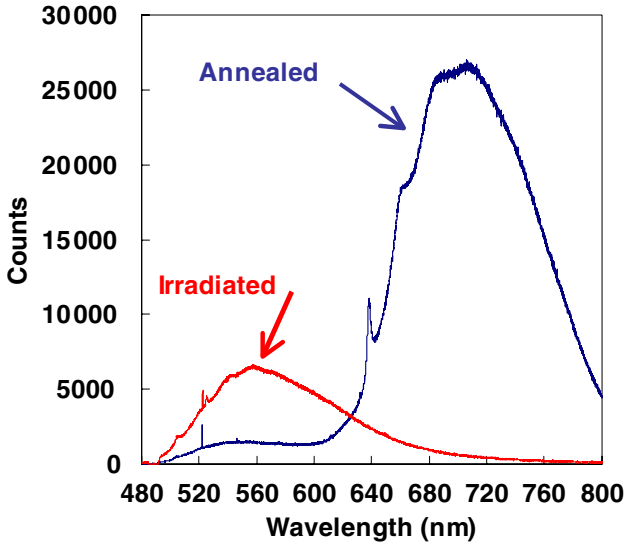

Fig. 5 (online colour). Photoluminescence spectra for a sample after irradiation, and after irradiation and annealing. The strong emission from NV^- is evident after the anneal

Table 1

Defect parameters and phase-memory times for the samples used in this work. The irradiations used electron energies of around 2 MeV. The NV^- concentrations were calculated from the fluences using [20]. The substitutional nitrogen concentrations come from EPR measurements. The phase-memory times are from electron–spin echoes

sample	electron fluence (cm^{-2})	$[NV^-]$ (ppm)	$[N_S]$ (ppm)	T_M (μs)
Apollo CVD	0	≤ 5	0.05	≥ 32
Sumi1	1×10^{16}	0.29	50	3.2
Sumi2	2.5×10^{16}	0.71	200	1.25
Sumi4	1×10^{17}	2.9	30	6.2
SumiR	7×10^{17}	20	200	3.6

Four HPHT samples from Sumitomo were irradiated and annealed to produce a set of samples in which the NV^- concentration varied by nearly a factor of 100. However, the phase-memory times for these samples varies only from 1.25 to 6.2 μs (Table 1). Since the variation is much smaller than what is expected by the simple law (Eq. (1)), the phase-memory time is not determined by the NV^- centers in these samples.

The substitutional nitrogen has an EPR spectrum that allows quantitative measurement of its concentration [17, 18]. At high concentrations the linewidth is proportional to $[N_S]$ due to dipolar broadening. At low concentrations, the linewidth is constant, arising from ^{13}C static dipolar coupling. In this work, the calibration from [18] was used in determining the N_S concentrations from EPR at 9 GHz. The four Sumitomo samples were analyzed along with an Apollo epitaxially grown CVD single crystal [19] (see Fig. 6). The Apollo CVD sample has a much lower $[N_S]$ than the HPHT diamonds (Fig. 6 and Table 1).

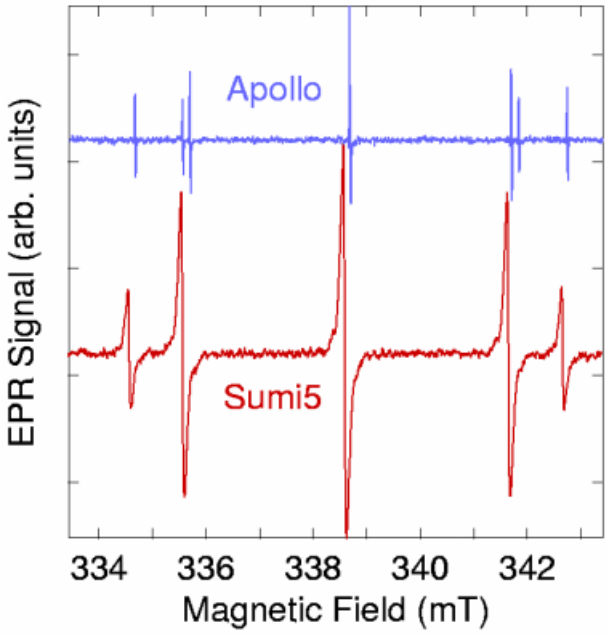

Fig. 6 (online colour). Room temperature EPR spectra taken at 9 GHz of N_S in two samples. The spectrum (often denoted as P1) arises from the hyperfine splitting from the $I = 1$ N-nuclei and is for fields near the [111]. The linewidth is sensitive to the concentration of N_S

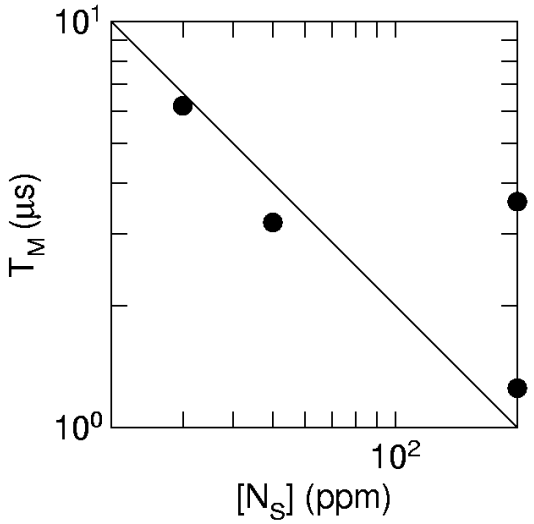

Fig. 7. Phase-memory times versus $[N_S]$ for Sumi samples. The line shows the expected inverse dependence of T_M on $[N_S]$

A good correlation is found for three of the Sumitomo samples (Fig. 7). For the fourth, the determination of $[N_S]$ was done independently [20], and this may explain the inconsistency with the others. The Apollo sample has a much lower $[N_S]$ and a much longer phase-memory time. These results show that phase-memory in the Sumitomo samples is controlled by the substitutional N. The straight line in Fig. 7 gives a value for k in Eq. (1) of 5×10^{-3} (μs ppm)$^{-1}$.

A few comments can be made to try to assess the state-of-the-art. First, the Apollo diamond exhibits a phase-memory time of at least 32 μs. Using the constant from the Sumitomo samples and Eq. (1), if the relaxation were by the substitutional N in this sample, the lifetime would be 4 ms. Refined measurements will be made to get the actual time for this sample. The longest reported phase-memory time for the NV^- center is 80 μs observed at low fields and a temperature of 1.4 K [21]. While the limit set by the ^{13}C nuclei has not been reached for the NV^- center, a limiting value of 1 ms was measured for N_S in diamond [18]. It is likely that the ^{13}C limit for NV^- is similar to this value.

3.2 ^{14}N and Multi-Bit Gates Having described the effect of distant electronic and nuclear spins on the quantum states, the focus now shifts to nuclei very close to the NV^- wave function. These include some of the ^{13}C that happen to be near a particular center and the ^{14}N that is a part of nearly every NV^-. In this work done near 1 T the conditions are such that effects of the nitrogen far outweigh the effects of nearby ^{13}C. In this section, the effects of ^{14}N are described with a suggestion for a CNOT gate.

The hyperfine interaction leads to additional splittings of the electronic ground state. These are shown schematically in Fig. 8a. For the Apollo sample the hyperfine splittings are resolved in the ODMR spectrum for microwave powers low enough to be free of power broadening (Fig. 8b). The hyperfine splitting was first reported by EPR [2] and has been studied in detail [22].

In addition to the hyperfine interaction, there is a strong anisotropic nuclear quadrupole interaction that can produce a coherent interaction between the electronic and nuclear spins when two conditions are met. First, the nuclear states must be mixed which occurs through the quadrupole interaction when the applied field is away from the symmetry axis of the defect, the [111]. Second, the microwave H-field must be large enough to cover two of the nuclear states. These conditions can be easily met and a

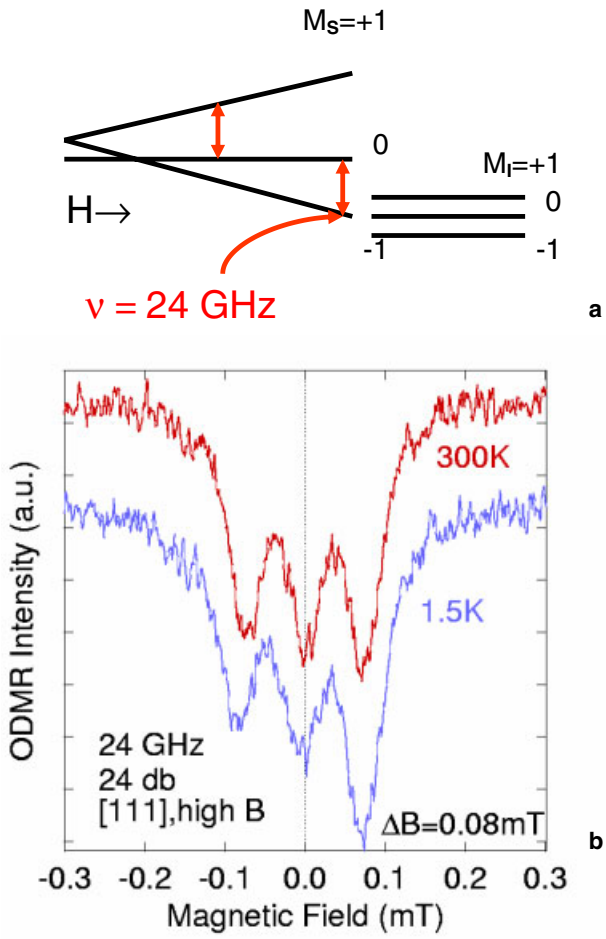

Fig. 8 (online colour). a) Schematic diagram showing the energy levels of the ground state with hyperfine splitting; b) the ODMR spectrum of the high-field transition at low microwave power for two temperatures. The different amplitudes in part b) indicate partial nuclear polarization

quantum beating is observed on the envelope of the echo decay (Fig. 9). In the language of spectroscopy, this effect is called Electron Spin Echo Envelope Modulation (ESEEM).

From the standpoint of single-qubit gates, the effects of the ^{14}N nuclear spin seem bad at first glance. However, since the electron spin and nuclear spin constitute a coupled pair, they could form the states for a two-qubit CNOT gate. The electronic spin could be the control bit and the nuclear spin the target bit with microwave and radio-frequency pulses to address each individually. This would lead to the sort of gate proposed and realized in liquid state NMR [14] in which spin-echo sequences are used to turn on and off the entanglement between the two spins. Such a demonstration with the NV^- center might require a higher magnetic field, a pure sample like the Apollo diamond, and a choice of the proper angle to optimize the electron–nuclear coupling. It does appear feasible.

Scaling to a large number of qubits within this concept would be a challenge. Quantum information proposals making use of Si and the III–V semiconductors have a large advantage when it comes to scaling due to the advanced state of the technologies based

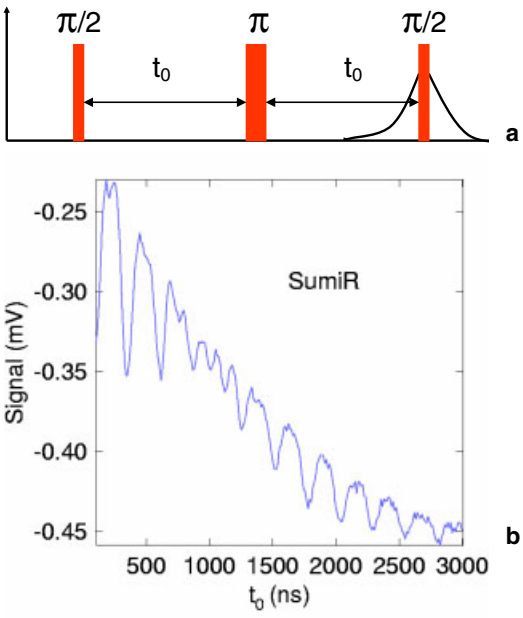

Fig. 9 (online colour). a) Schematic of the pulse sequence for generating an echo decay; b) the echo decay for a Sumi sample with the field in the [110]. Strong beating from ^{14}N nuclear spin states is observed

on these materials. Efforts are being made for scaling in diamond, however. For example, patterns of NV^- centers have been written with focused-ion beams to a resolution of less than 1 μm [23].

4. Conclusion Building on the excellent optical and spin properties of the NV^- center in diamond, a concept of single-qubit gates for quantum information technology has been demonstrated. The electronic spin of the ground state of the NV^- centers acts as the qubit. The state is optically polarized and optically detected. Microwave pulses operate on the state. Although the demonstration made use of ensembles, the extension to single NV^- centers seems possible.

This defect-host system exhibits very long coherence times in the solid-state. Decoherence is set by different mechanisms with different limits. HPHT diamonds contain a high concentration of dispersed N that limits the phase-memory to a few μs. A single-crystal CVD diamond shows a lifetime of at least 32 μs and the best reported time is 80 μs [21]. The relaxation from ^{13}C nuclei in natural abundance is expected to set a limit around 1 ms.

The spin from the ^{14}N nucleus in the NV^- center is strongly coupled to the electronic spin and, under certain conditions, influences its quantum state. However, this spin and its coupling could be used for a demonstration of a CNOT gate with the NV^- center.

Acknowledgements This work was supported in part by the Naval Research Laboratory/Office of Naval Research. F.T.C. was an NRC-NRL Research Associate and J.S.C. is currently an NRC-NRL Research Associate. We thank S. C. Rand, M. K. Bowman, G. D. Watkins, D. C. Look, G. Farlow, and R. Eisinger for their contributions to this work.

References

[1] G. Davies and M. F. Hamer, Proc. R. Soc. London A **348**, 285 (1967).
[2] J. H. N. Loubser and J. A. van Wyk, Diamond Res. **11**, 11 (1977).
[3] E. van Oort, N. B. Manson, and M. Glasbeek, J. Phys. C **21**, 4385 (1988).
[4] K. Holliday, X.-F. He, P. T. H. Fisk, and N. B. Manson, Opt. Lett. **15**, 983 (1990).
[5] A. Gruber, A. Draebenstedt, C. Tietz, L. Fleury, J. Wrachtrup, and C. von Borczyskowski, Science **276**, 2012 (1997).
[6] J. Wrachtrup, S. Ya. Kilin, and A. P. Nizovtsev, Opt. Spectrosc. **91**, 429 (2001).

[7] M. S. SHARIAR, J. A. BOWERS, B. DEMSKY, P. S. BHATIA, S. LLOYD, P. R. HEMMER, and A. E. CRAIG, Opt. Commun. **195**, 411 (2001).
[8] C. KURTSIEFER, S. MAYER, P. ZARDA, and H. WEINFURTER, Phys. Rev. Lett. **85**, 290 (2000).
[9] A. BEVERATOS, R. BROURI, T. GACOIN, J.-P. POIZAT, and P. GRANGIER, Phys. Rev. A **64**, 061802 (2001).
[10] F. T. CHARNOCK and T. A. KENNEDY, Phys. Rev. B **64**, 041201 (2001).
[11] D. P. DIVINCENZO and D. LOSS, Superlattices Microstruct. **23**, 419 (1998).
[12] J. WRACHTRUP, C. VON BORCZYSKOWSKI, J. BERNARD, M. ORRIT, and R. BROWN, Phys. Rev. Lett. **71**, 3565 (1993).
[13] A. P. NIZOVTSEV, S. YA. KILIN, C. TIETZ, F. JELEZKO, and J. WRACHTRUP, Physica B **308–310**, 608 (2001).
[14] N. A. GERSHENFLED and I. L. CHUANG, Science **275**, 350 (1997).
[15] See, for example, Properties and Growth of Diamond, Ed.: G. DAVIES, INSPEC, 1994.
[16] I. M. BROWN, in: Time Domain Electron Spin Resonance, Eds. L. KEVAN and R. N. SCHWARTZ, John Wiley & Sons, New York 1979.
[17] J. ISOYA, C. P. LIN, M. K. BOWMAN, J. R. NORRIS, S. YAZU, and S. SATO, in: Science and Technology of New Diamond, Proc. 1st Internat. Conf. New Diamond Science and Technology, Tokyo (Japan), 1988, Ed. S. SAITO, KTK-Terra, 1990 (p. 357–361).
[18] J. A. VAN WYK, E. C. REYNHARDT, G. L. HIGH, and I. KIFLAWI, J. Phys. D **30**, 1790 (1997).
[19] R. LINARES and P. DOERING, Diam. Relat. Mater. **8**, 909 (1999).
[20] A. LENEF, S. W. BROWN, D. A. REDMAN, and S. C. RAND, Phys. Rev. B **53**, 13427 (1996).
[21] M. GLASBEEK and E. VAN OORT, Radiat. Eff. Defects Solids **119–121**, 301 (1991).
[22] N. B. MANSON, X.-F. HE, and P. T. H. FISK, Opt. Lett. **15**, 1094 (1990).
[23] J. MARTIN, R. WANNEMACHER, J. TEICHERT, L. BISHOFF, and B. KOEHLER, Appl. Phys. Lett. **75**, 3096 (1999).